IEEE Access
Multidisciplinary | Rapid Review | Open Access Journal

Received November 13, 2021, accepted December 14, 2021, date of publication December 20, 2021,
date of current version December 28, 2021.

Digital Object Identifier 10.1109/ACCESS.2021.3136817

Wireless Power Transfer Based on Spider Web–Coil for Biomedical Implants

AMAL IBRAHIM MAHMOOD[1,2], SADIK KAMEL GHARGHAN[2], (Member, IEEE), MOHAMED A. A. ELDOSOKY[1], MUSTAFA FALAH MAHMOOD[2], AND AHMED M. SOLIMAN[1]

[1]Biomedical Engineering Department, Faculty of Engineering, Helwan University, Helwan, Cairo 11792, Egypt
[2]Middle Technical University, Electrical Engineering Technical College-Baghdad, Iraq

Corresponding author: Sadik Kamel Gharghan (sadik.gharghan@mtu.edu.iq)

This work was supported in part by the Biomedical Engineering Department, Faculty of Engineering, Helwan University, Cairo, Egypt; and in part by the Department of Medical Instrumentation Engineering Techniques, Electrical Engineering Technical College, Middle Technical University.

ABSTRACT A biomedical implant (BMI) is a device that allows patients to monitor their health condition at any time and obtain care from any location. However, the functionality of these devices is limited because of their restricted battery capacity, such that a BMI may not attain its full potential. Wireless power transfer technology–based magnetic resonant coupling (WPT–MRC) is considered a promising solution to the problem of restricted battery capacity in BMIs. In this paper, spider web coil–MRC (SWC-MRC) was designed and practically implemented to overcome the restricted battery life in low–power BMIs. A series/parallel (S/P) topology for powering the BMI was proposed in the design of the SWC-MRC. Several experiments were conducted in the lab to investigate the performance of the SWC-MRC system in terms of DC output voltage, power transfer, and transfer efficiency at different resistive loads and distances. The experimental results of the SWC-MRC test revealed that when the V_{source} is 30 V, the DC output voltage of 5 V can be obtained at 1 cm. At such a distance (i.e., 1 cm), the SWC-MRC transfer efficiency is 91.86% and 97.91%, and the power transfer is 13.26 W and 23.5 W when 50- and 100-Ω resistive loads were adopted, respectively. A power transfer of 12.42 W and transfer efficiency of 93.38% were achieved at 2 cm for when a 150-Ω resistive load and a V_{source} of 35 V were considered. The achieved performance was adequate for charging some BMIs, such as a pacemaker.

INDEX TERMS Biomedical implant, MRC, power transfer, transfer efficiency, voltage, WPT.

I. INTRODUCTION

Biomedical implant (BMI) systems depend on the type of electronic device implanted to enhance the quality of life as well as to observe, diagnose, and substitute the function of an organ or bodily function without restricting the patient's movement [1], [2]. Generally, a BMI is either biodegradable or powered by limited-storage internal batteries or supercapacitors. Therefore, the patient should replace the implant battery before it is depleted [3], [4]. The need for repeated replacement is impractical and requires a high cost to patients due to surgical intervention [5]. Wireless power transfer (WPT) involves transferring electrical energy from the transmitter to the receiver ends without using wires. These WPTs can be divided into two categories based on the coupling region between the transmitter and receiver: (i) non–radiative or near–field region and (ii) radiative or far-field region [6], [7].

Near-field WPT can be classified into four categories relying on the coupling technique employed: (i) inductive coupling (IC), (ii) magnetic-resonant coupling (MRC), (iii) magneto-dynamic coupling (MDC), and (iv) capacitive coupling (CC). The use of WPT plays an essential role due to its safety, comfortability, and flexibility for patients. Due to technological advancements, WPT can be used in several applications, including electric vehicles, mobile phones, wearable electronics, and BMI systems [8]–[10]. Wireless power transfer plays an important part in BMI systems, as it is free from wires and negates the need for surgery when the battery is depleted. To enhance the resulting power-transfer efficiency and coupling between transmitter and receiver coils of WPT for BMI devices, researchers proposed

The associate editor coordinating the review of this manuscript and approving it for publication was Tariq Masood.

several techniques and methods: coil geometry [11]–[13] different closed–loop and open–loop power control [14], power amplification [15], [16] an impedance-matching network [17], [18] misalignment conditions [19], and coupling configuration [20], [21]. In the biomedical field, WPT is essential as an energy source for biosensing and BMI devices [22] such as vital human–signs monitoring [23], heart-rate sensors [24], capsule endoscopy [25], left ventricular assist devices (LVAD) [26], deep micro-implants [27], and optogenetics applications [28].

In WPT applications, most of the research, either in vivo or in vitro, applied the systems for different transfer distances, loads, coupling topology, and adopted techniques. In each condition, the delivered power and transfer efficiency are different. The distance between the coils is affected by mutual inductance [20]. Then, the change in mutual inductance affected the ability of power transfer and power transfer efficiency [30]. Hence, the transmitter and receiver circuit can be tuned to the resonance angular frequency (ω°) to optimize the power-transfer efficiency [31]. However, the MRC is an appropriate technique for midrange distances, and its power transfer and efficiency rely on the size and shape of the receiver and transmitter coils [5]. Therefore, the MRC is suitable for BMI systems. The transfer efficiency and power of the MRC technique can be improved by adopting the suitable type and size of transmitter and receiver coils as well as the connection method of resonance capacitors with the coils. However, the value of these capacitors determines the resonance frequency ($\omega_{\circ}$). The capacitor configuration involves many coupling-capacitor topologies such as series/series (S/S), series/parallel (S/P), parallel/parallel (P/P), and parallel/series (P/S) [32], [33].

Depending on the function of the WPT system, the resonance frequency, transfer distance, coil size, resistance load, voltage, and compensation topology can be determined to achieve optimum transfer efficiency. On the primary side of the system, the series topology should be investigated to attain distance transmission. For high current, the parallel configuration must be considered. Moreover, if the demand requirement has voltage-source criteria, the secondary side can be designed with the series compensation. Otherwise, a parallel compensation is chosen to attain the current source criteria [9], [32]. In the proposed study, the S/P topology is adopted to achieve a good transfer distance and current source characteristics suitable for BMI battery charging. This study differs from other studies by designing a spider web coil–MRC (SWC-MRC), which can be considered a rare method in BMI design. Also, the use of S/P topology in SWC-MRC improves the delivered power for a few centimeters of air gaps.

The contributions of the current study can be summarized as follows:

1) The use of SWC-MRC entails an S/P configuration and was designed and implemented practically for medical implant devices.
2) Several performance metrics of the proposed SWC-MRC, such as DC output voltage, power transfer, and efficiency, were analyzed concerning source voltage and distances at different resistive loads to produce the best value of the DC output voltage.
3) The SWC-MRC was successful in achieving a sufficient DC output voltage that can be used for charging the battery of BMI devices powered by 5 V.
4) The performance metrics of SWC-MRC have outperformed the relevant literature in terms of power transfer, efficiency, and air gap between the coils of the system.

II. RELATED WORKS

Much research exists that addresses the use of MRC-WPT in many fields in electronics, including BMI devices. Kim *et al.* [34] designed a WPT system for cardiac-monitoring BMI devices that has low thermal radiation. The proposed system involves many turns configured in an S/P topology. The researchers found that a 24% transfer efficiency can be achieved with only a 10-mm air gap. Their results showed that the temperature of the WPT system increased only 2°C during a 70-min charging, making it a safe system. Peng *et al.* [35] introduced an optimal design method for BMIs using a capacitive L–matching network, indicating a transfer efficiency of 36.43% at a 15-mm air gap when an oscillating frequency of 6.78 MHz is adopted. The coupling between the two coils was loose, and the coupling factor k was 0.035.

Kim *et al.* [36] used an S/P configuration to achieve an efficient design used for implantable electrocardiograph (ECG) monitoring with a charging voltage of 4.2 V and a transfer efficiency of 10%. This design can record and transmit ECG data for 23 hours without recharging the battery. The design's limitation is its sensitivity to AC power–line 60-Hz noise. Heo *et al.* [37] developed a wireless sensor applied as an ECG sensor using the magnetic induction–type WPT method. The alignment position between receiver and transmitter coils and the power transmission efficiency had been considered. The actual experimental system involved a circular transmitter coil with a diameter of 5 cm and an elliptical receiver coil with a long axis. The system was compared with the high-frequency structure simulator (HFSS) system. The result shows that the delivery of voltage by the receiver coil is 4.8 V. The transmission efficiency is 1.5% when the distance between the transmitter and receiver is less than 2 cm. The simulation result shows that the transmission efficiency remains stable even if the alignment between the transmitter and receiver changes.

Moreover, Yazdi *et al.* [38] introduced an inductive WPT system with three elliptical, circular, and square designs to improve transfer efficiency in implantable ECG sensors. Six different coil configurations are suggested: circular-circular, an elliptical-elliptical, an elliptical-square spiral coil, a circular-square spiral, a circular-elliptical, and a square

spiral-square spiral. The results indicate that the maximum transfer efficiency is achieved when the transfer distance is 0 mm and the design is a square spiral-square spiral. The adopted oscillating frequency is 13.56 MHz. The advantage of this work compares to many types of coil designs, but the obtained transfer distance is small.

Dubey *et al.* [39] suggested that a 1.3-MHz resonant wireless-powered gastric simulator provided an electrical pulse with suitable power and indicated that the efficiency of such a system was 14% when the transfer distance was 4 cm at 500-Ω resistive load. The misalignment effect of the system was investigated. The limitation of the work is that it is not validated experimentally. To enhance the efficiency and stability of the capsule endoscope, Cui *et al.* [40] introduced a new system with six Helmholtz coils as transmitters. The researchers studied the effect of receiver position on the coupling factor. The complexity of the setup limited the design configuration, but the system can generate a high-intensity magnetic field that enhances the system's transfer efficiency even when the coils are misaligned.

Fadhel *et al.* [41] designed a modified WPT system. The design comprised a high-efficiency complementary metal-oxide-semiconductor component and an optimized printed circuit coil. The system involves a transmitter designed with an oscillator, driver, and a class-E power amplifier; the receiver contains a circular spiral coil. When the transmitting medium is air at transfer distances of 0.5 cm and 5 cm, experimental results showed that the power transfer efficiency is 75.1% and 10.67%, respectively. The receiver coil received power for 0.5 cm and 5 cm at 157.7 mW and 22.4 mW, respectively. The results indicate that the system applies to transcutaneous applications that need a short transfer range. Therefore, the proposed system has a small, delivered power for an air gap of a few centimeters.

Xu *et al.* [42] implemented a novel, efficient, and miniaturized magnetic resonance WPT system for implantable BMI devices based on a flexible, three-dimensional dual coil. Then, the authors analyzed the factors affecting transmission efficiency. The system is composed of a signal source, an impedance-matching module, a double coil–coupled resonant module, a receiver circuit, and a load. The simulated software used is HFSS. The effect of the coil's structural parameter was analyzed, and the coil's optimization structure was obtained. The resulting analysis shows that maximizing coil inductance resulted in enhanced transfer efficiency. The achieved delivery output power is 70 mW when the transfer distance is 6 mm, the input power is 200 mW, and the maximum transfer efficiency is 35%. Therefore, the system has small transferred power over a low-transfer distance.

As the dimension of the receiver coil has an important role in the design, Ibrahim *et al.* [43] suggested a wireless-power transmission link including a printed spiral coil to power a millimeter-sized BMI. The oscillating frequency of the setup was determined at 50 MHz and 100 MHz. The optimized design had a transfer efficiency of 0.13% and 3.3%, respectively. The delivered power was 65.7 μW and 720 μW at 10 mm, respectively. The results indicate that the system has low power and a small transfer distance, but the design is useful for millimeter-sized BMIs. Knecht *et al.* [44] designed a high-efficiency WPT system that utilizes gallium-nitride (GaN) semiconductor technology to limit power loss in mechanical circulatory support–system devices such as an LVAD. They found that the optimized transmitting power is 30W, and transfer efficiency is 95% at a 20-mm transfer distance.

Shadid *et al.* [45] introduced a hybrid wireless-power and data-transfer system for medical implants consisting of an antenna and coil. The antenna is characterized by operating with three different frequencies: 415 MHz, 905 MHz, or 1,300 MHz. The coil is designed to transfer power at a resonance frequency of 13.56 MHz. The authors also studied WPT using a wearable antenna. The system achieved a high transfer efficiency of 72.26% at a small transfer distance of 15 mm. Haerinia *et al.* [46] presented a far-field system to work on 2.5 GHz and 4.5 GHz bands involving a dual-band–printed planar antenna. They examined the specific absorption rate value. Sallan *et al.* [47] used Neumann's equation to introduce a mathematical model for calculating inductively coupled coils of L_{Tx}, L_{Rx}, and M. Abou Houran *et al.* [48] reviewed the main development of the MRC-WPT system by discussing many parameters, such as compensation topologies, misalignment, and structure of the resonators.

From the aforementioned articles, we deduce that the power delivery, transfer efficiency, transfer distance, and coil size of WPT in BMI systems are facing challenges and limitations. Therefore, in this study, we try to solve these issues by adopting a new design of SWC-MRC. Thereby, the delivered output power and efficiency within a specific distance can be improved and supply some BMI devices with sufficient voltage.

III. RESEARCH METHODOLOGY

To overcome the limitation of battery capacity in BMIs, the materials and methods introduced in this work involve the design and implementation of the SWC-MRC system to solve the problem of charging BMI batteries wirelessly. The proposed SWC-MRC design involves using an S/P coil topology based on spider-web coils to analyze different performance metrics, including DC output voltage, transferred power, and transfer efficiency. The adopted SWC-MRC design can be experimentally implemented and tested at different resistive loads. The transfer distance between transmitter and receiver coil is 1-10 cm in every 1-cm step. The transmitter coil was fixed during measurement, while the receiver location was varied.

Different power supply values were adopted in the experiment, ranging between 5-60 V in a 5-V step for each case to explore which voltage provides the best performance. A comparison was made between each supply and at each distance. The previously mentioned materials and methods can be used assuming the following:

1) The spider web–coil form was designed with an inner diameter of 10.5 cm and an outer diameter of 24 cm. The form is fabricated on clear polyvinyl chloride sheets as shown in Fig. 1a.
2) A copper coil with the dimension of 20 America–wire gauge (AWG) in diameter was manually wrapped above the spider coil form. Four turns were wrapped on the transmitter spider-web form. The receiver was wrapped in three turns, as clarified in section 4 (Fig. 1b and 1c, respectively).
3) All required devices and tools were prepared for both the transmitter and receiver side as described in section 4.
4) Simple mathematical models were used to calculate the delivered power measured in watts (W), and a percentage of transferred efficiency was introduced to analyze the performance metrics of the SWC-MRC as clarified in section 5.
5) The SWC-MRC design was presented to provide adequate voltage to charge a BMI. The SWC-MRC contains the transmitter and receiver parts. Each part involves a specific device and tools to meet the required aims of the work.
6) As the overall design component was prepared, three experiments were configured and conducted to evaluate the performance of SWC-MRC according to the load. The system design and parameters were explained in detail.
7) An analysis of each experiment was introduced, and the results were described.

IV. SYSTEM DESIGN

The proposed SWC-MRC system consists of a transmitter and receiver parts. The transmitter contains two power supplies: a high-efficiency zero voltag–switching (ZVS) differential-mode class-D power amplifier based on development board EPC9065, and a spider-web transmitter coil to convert an electrical field to a magnetic field with a compensated capacitor ($_{CT}$x). The receiving part includes a spider web–receiver coil to convert the magnetic field to an electrical signal, $_{CR}$x, a bridge rectifier (based on Schottky-diodes) characterized by its small size and low cost, capacitance filter (C), and resistive load (RL).

The key to the design of the system is the spider web–coils of the transmitter and receiver, as shown in Fig. 1. The direct current (DC) generated by the power supply is converted to a sinusoidal alternating-current (AC) wave with an oscillator frequency of 6.78 MHz using ZVS [49] from GaN-based power management technology as shown in Fig. 2a and 2b. This frequency was selected because at high frequency, especially in the Industrial, Scientific, and Medical (ISM) band (2.2 and 6.78 MHz), the output power could be small, and the BMI does not require an extra electronic circuit [7]. In addition, this frequency (i.e., 6.78 MHz) reduces the eddy current effect in the receiver circuit, hence the WPT efficiency can be improved. Furthermore, decreasing the eddy currents will reduce the temperature of the receiving circuit implanted in the human body will decrease, which prevent side effects on the tissues and cells of the body. The ZVS is connected directly to the transmitter circuit. The current flows through the transmitter (Tx) coil, resulting in an electromagnetic field passing through the receiver (Rx) coil. Therefore, the Rx coil produces an induced current to perform the wireless-energy transmission from the Tx coil to the Rx one.

The transferred energy from the Tx to the Rx coils suffers some loss. Therefore, the current in the Rx coil is smaller than that of the Tx coil. The Tx side involves a bridge rectifier to convert AC to DC, which is usable power. The Tx and Rx coils should resonate at the same frequency to obtain an efficient power transfer. Fig. 3 shows the circuit of the proposed system. This technique is characterized by its high-transfer efficiency that is unaffected by the environment [23]. The main parameters of the SWC-MRC design are included in Table 1.

V. MATHEMATICAL MODEL FOR S/P TOPOLOGY

The proposed work involves an SWC-MRC setup with S/P topology as shown in Fig. 3. The resonance frequency of the transmitter coil and receiver coil is ωTx and ωRx, respectively, and is equal to ω°, which is 6.78 MHz. The system works in the S/P configuration. The proposed system was tested with an air gap ranging from 1-10 cm separating the transmitter coil and receiver coil. Several induced voltages ranging from 5-60 V were used to test the system. As shown in Fig. 3, Us, L_{Tx}, C_{Tx} represent the voltages obtained from the oscillator, transmitter-coil inductance, and transmitter-compensation capacitor, respectively. The L_{Rx} and C_{Rx} indicate the receiver-coil inductance and receiver-compensation capacitor, respectively. The values of C_{Tx} and C_{Rx} can be calculated using equations 1, 2, and 3 [50], [51].

$$\omega_{\circ} = \frac{1}{\sqrt{L_{TX}C_{TX}}} = \frac{1}{\sqrt{L_{RX}C_{RX}}} \tag{1}$$

$$C_{TX} = \frac{1}{L_{TX}\omega_o^2} \tag{2}$$

$$C_{RX} = \frac{1}{L_{RX}\omega_o^2} \tag{3}$$

In this work, L_{Tx} and L_{Rx} are 10 μH and 5 μH, respectively, at 6.78 MHz according to equations 2 and 3. The values of the adopted ceramic capacitors C_{Tx} and C_{Rx} are

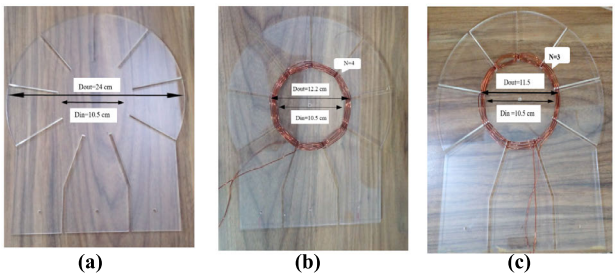

(a) (b) (c)

FIGURE 1. Spider web–coil form for the proposed SWC-MRC system: (a) spider-web coil form (b) transmitter coil and (c) receiver coil.

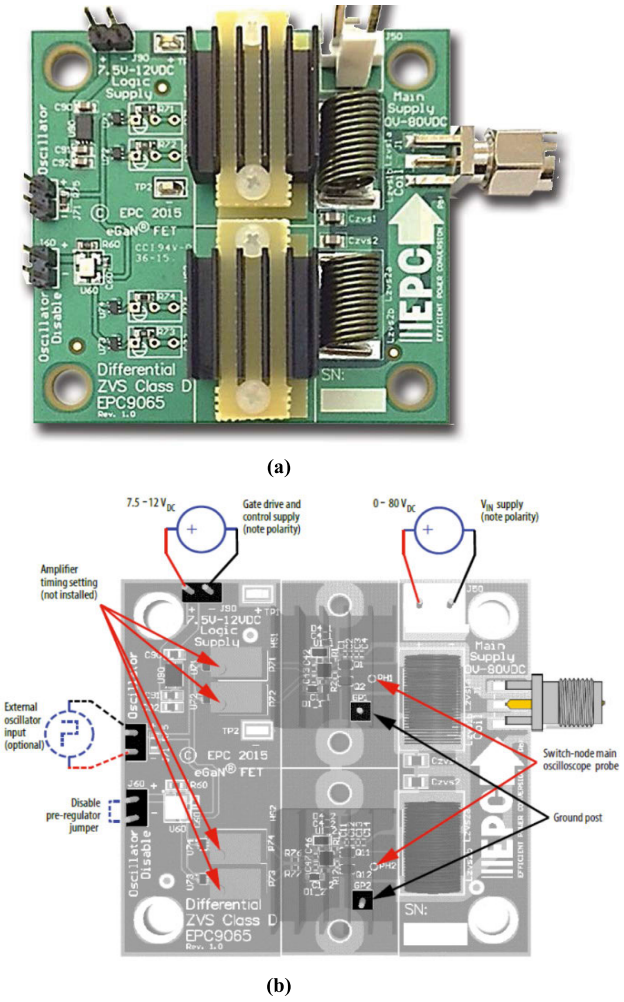

FIGURE 2. GaN-based power management technology: (a) An EPC9065 amplifier board and (b) Proper connection and measurement setup for the amplifier board [49].

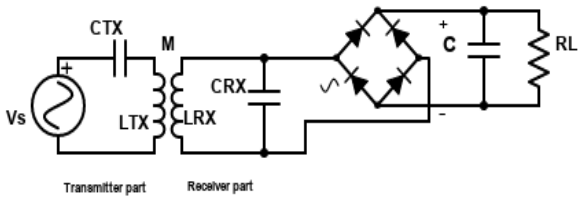

FIGURE 3. Schematic diagram of the proposed SWC-MRC system using S/P topology.

55 picofarads (pF) and 110 pF, respectively. The outer diameter of the transmitter coil (d_{Tx}) is 12.2 cm, and the outer diameter of the receiver (d_{Rx}) is 11.5 cm. The induced and reflected voltage is described by mutual inductance M and the operation frequency ω_o. The value of M is determined by inducing an electromotive force in the receiver coil by changing the current through it. The value of M between L_{Tx} and L_{Rx} is calculated using equation 4 [31] as follows:

$$M = \frac{\mu_o \pi \left(d_{TX} d_{RX}\right)^2 N_{TX} N_{RX}}{2\sqrt{\left(d_{RX}^2 + X^2\right)^3}} \tag{4}$$

TABLE 1. Parameters of the SWC-MRC system.

Parameters	Symbol	Transmitter Coil	Receiver Coil
Operating frequency	f (MHz)	6.78	6.78
T_x inductance	L_{Tx} (μH)	10	___
R_x inductance	L_{Rx} (μH)	___	5
T_x No. of turn	N_{Tx}	4	___
R_x No. of turn	N_{Rx}	___	3
T_x Capacitor	C_{Tx} (pf)	55	___
R_x Capacitor	C_{Rx} (pf)	___	110
Outer diameter	D_{out} (cm)	12.2	11.5
Inner diameter	D_{in} (cm)	10.5	10.5
Wire thickness	w (mm)	0.8128	0.8128
Weight	(gm)	23.89	16.85

where μ_o is the permeability of free space ($4\pi \times 10^{-7}$) [52], N_{Tx} and N_{Rx} are the number of turns in the transmitter coil and receiver coil, respectively. The value for X is the air-gap distance between the transmitter and receiver coils.

Moreover, when the reactive impedance of the coil in the S/P configuration becomes zero and the reactance of the coil is close to zero, resonance occurs [53]. The receiver coil penetrated by a specific amount of magnetic flux represented by coupling coefficient k can be measured by equation 5 [54] as follows:

$$k = \frac{M}{\sqrt{L_{TX} L_{RX}}} \tag{5}$$

The delivered output power was calculated using equation 6, and the power transfer efficiency was calculated using equation 7 [55], [56].

$$output\ power = voltage \times current \tag{6}$$

$$Efficiency = \frac{P_{out}}{P_{in}} \times 100\% \tag{7}$$

The voltage and current in equation 6 are the load voltage and the load current, respectively. In equation 7, P_{out} represents the delivered power, and P_{in} is the input power. Both P_{out} and P_{in} are measured in watts.

VI. EXPERIMENTAL SETUP

In this study, the SWC-MRC configuration was used. Three experiments were conducted based on S/P topology to evaluate the performance of the SWC-MRC. The experiment block diagram illustrated in Fig. 4 identifies the main system components. The experimental setup of the proposed SWC-MRC design was configured to investigate the performance of the suggested work related to DC output voltage, transferred power, power-transfer efficiency, and the air gap between the transmitter and receiver coils. In this setup, the ZVS is based on development board EPC9065 operation but was not

limited to the lowest industrial, scientific, and medical band with an operating frequency of 6.78 MHz. The EPC9065 board involves two DC power supplies for both the oscillator and the gate of the enhancement mode GaN transistors (eGaN FETs) drive. The gate drive is responsible for supplying power to the class-D power amplifier. Based on the EPC9065 sheet guide [49] the gate drive and control supply must range between 7.5 V DC and 12 V DC. The voltage supply of the EPC9065 board must not exceed 80 V.

In this study, the gate drive supply is fixed at 8 V, which is adequate to operate the drive. The adopted voltage supply is between 5 V and 60 V. The system was examined for different distances ranging from 1-10 cm at every 1-cm step. Three resistor loads—50 Ω, 100 Ω, and 150 Ω—were investigated for each value of voltage supply and distance. At first, the DC output voltage was measured when the transferred distance was 1 cm, the voltage supply was 5 V, and the resistive load was 50 Ω. In addition, the delivered power and the power-transfer efficiency were calculated based on the measurements of DC output current and voltage. The distance was increased one step (i.e., 1 cm), and the same parameters were investigated until the 10-cm air gap was reached.

The steps mentioned earlier were performed again for the other voltage value until 60 V was reached. Fig. 5 shows the experimental setup of the proposed SWC-MRC system.

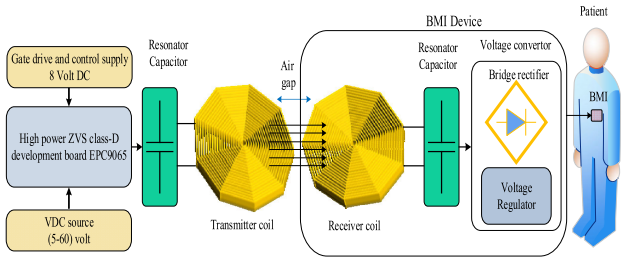

FIGURE 4. Main system components of the SWC-MRC experiment.

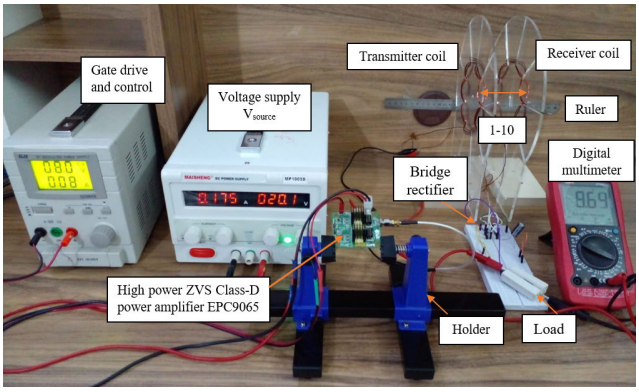

FIGURE 5. Experimental setup of the proposed SWC–MRC system.

VII. RESULT AND DISCUSSION

In this section, we introduce findings from implementing our proposed SWC-MRC system converting AC to DC and analyzing the DC output voltage, delivered output power, and power-transfer efficiency as a function of applied voltage supply V_{source} within a specific range of transfer distance. We gradually increased the transfer distance between the transmitter and receiver coils from 1-10 cm by 1-cm steps to determine the maximum DC output voltage, delivered output power, transfer efficiency, and transfer distance that can be reached by this SWC-MRC system. Three different resistive loads (50 Ω, 100 Ω, and 150 Ω) were considered for each test because these values were recommended in several research works [12], [35].

A. RESULTS OF DC OUTPUT VOLTAGE

In the proposed SWC-MRC system, DC output voltages were measured using a multimeter. The V_{source} was varied from 5-60 V stepwise by 5 V. The DC output voltage was measured for each value of V_{source} for three cases of resistive load. Moreover, measurements were obtained for different transfer distances between the transmitter and receiver coils. This transfer distance ranged from 1-10 cm stepwise by 1 cm. The change in V_{source}, in volts, is plotted on the x-axis; the obtained DC output voltage, in volts, is plotted on the y-axis, as shown in Fig. 6. As the V_{source} increases from 5-60 V, the DC output voltage also increases for the same distance. It was noted that the best performance is obtained at small distances. For example, the DC output voltage was 12.3 V when the V_{source} was 30 V, and the air gap between the transmitter and receiver coils was 2 cm when the system was loaded by 50 Ω as shown in Fig. 6a. However, the DC output voltage drops when the distance is less than 1 cm, and the V_{source} was 30 V at a resistive load of 50 Ω. This occurs due to the heat increase across the transmitter coil.

Fig. 6 shows that there is no DC output voltage after 30 V of V_{source}, because the DC output voltage is reduced to minimum values when the air gap is less than 2 cm. Whereas, the measured DC output voltage was 20.4 V and 26.5 V, respectively, for the same conditions of the air gap and V_{source} when the system is loaded by 100 Ω and 150 Ω. On the contrary, the DC output voltage is dropped at 2 cm and 3 cm, respectively, when the proposed system is loaded with 100 Ω and 150 Ω and the V_{source} is more than 40 V. The performance of the SWC-MRC can be investigated at a DC of 5 V, where this voltage can be employed to supply power to a BMI device. The DC output voltage of 5 V can be performed of 6 cm, 8 cm, and 9 cm at 50 Ω (Fig. 6a), 100 Ω (Fig. 6b), and 150 Ω (Fig. 6c), respectively, when the V_{source} is 60 V.

B. RESULTS OF DELIVERED OUTPUT POWER

A BMI working properly requires electrical power to maintain its activity. Depending on BMI applications, the required power of a BMI ranges from a few microwatts to tens of milliwatts. However, the battery specification is limited by its capacity and lifetime, making surgical replacement a basic disadvantage to this BMI. In our proposed SWC-MRC system, the measured power transfer at three different loads is studied, as illustrated in Fig. 7. The delivered power was calculated according to equation 6 in section 5.

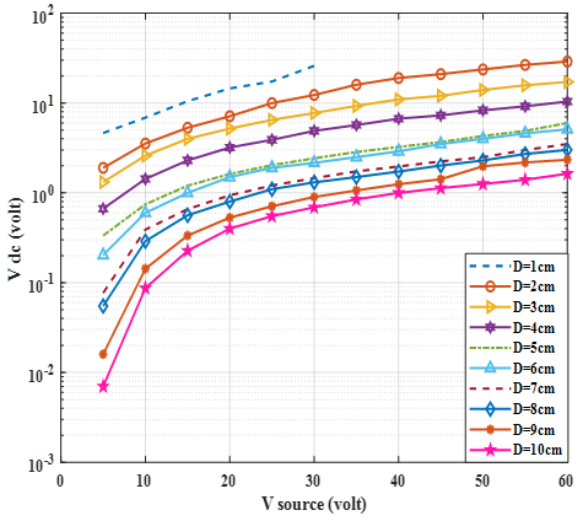

(a)

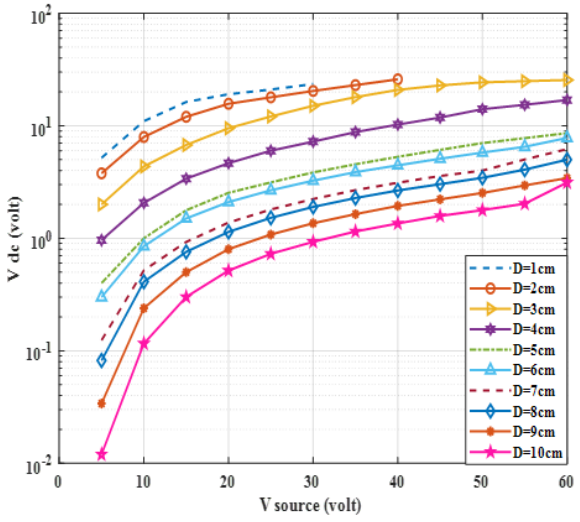

(b)

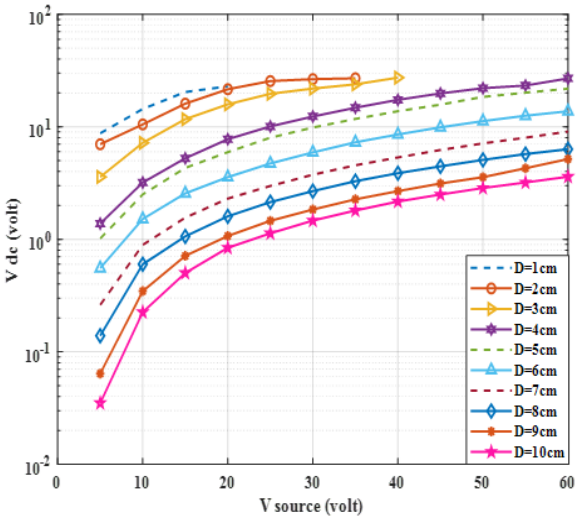

(c)

FIGURE 6. The performance of DC output voltage against different input voltages for air gaps ranging from 1-10 cm at different resistive loads: (a) 50Ω, (b) 100Ω, and (c) 150Ω.

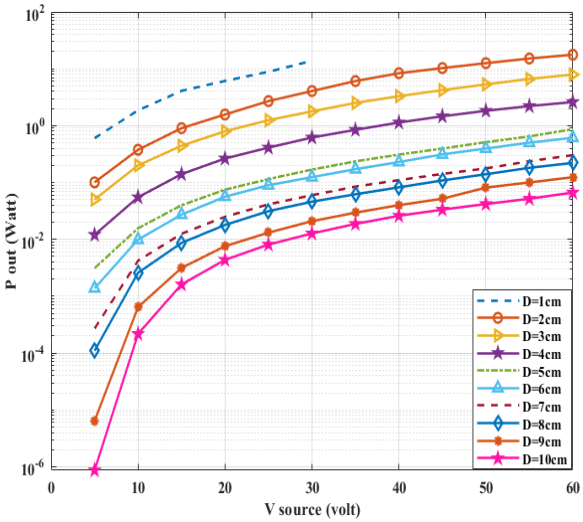

(a)

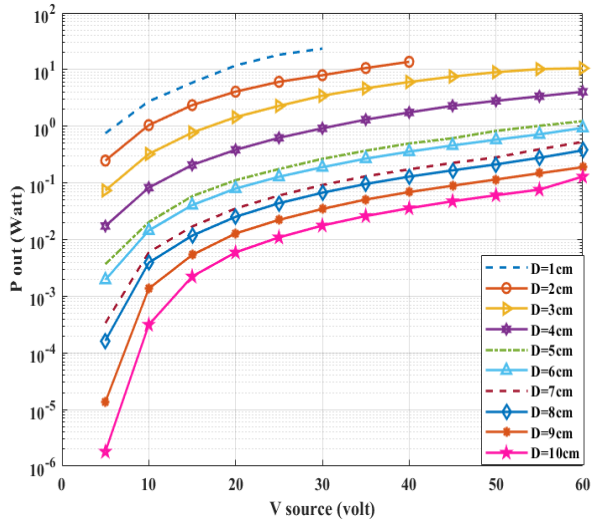

(b)

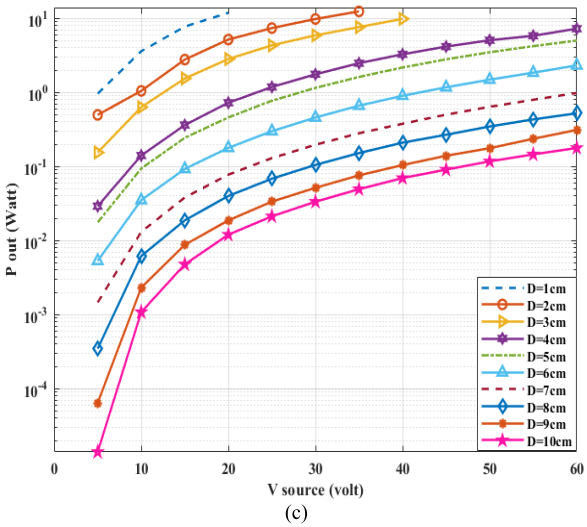

(c)

FIGURE 7. Delivered power on the receiver side is relative to different input voltages for the air gap ranging from 1-10 cm at different resistive loads: (a) 50 Ω, (b) 100 Ω, (c)150 Ω.

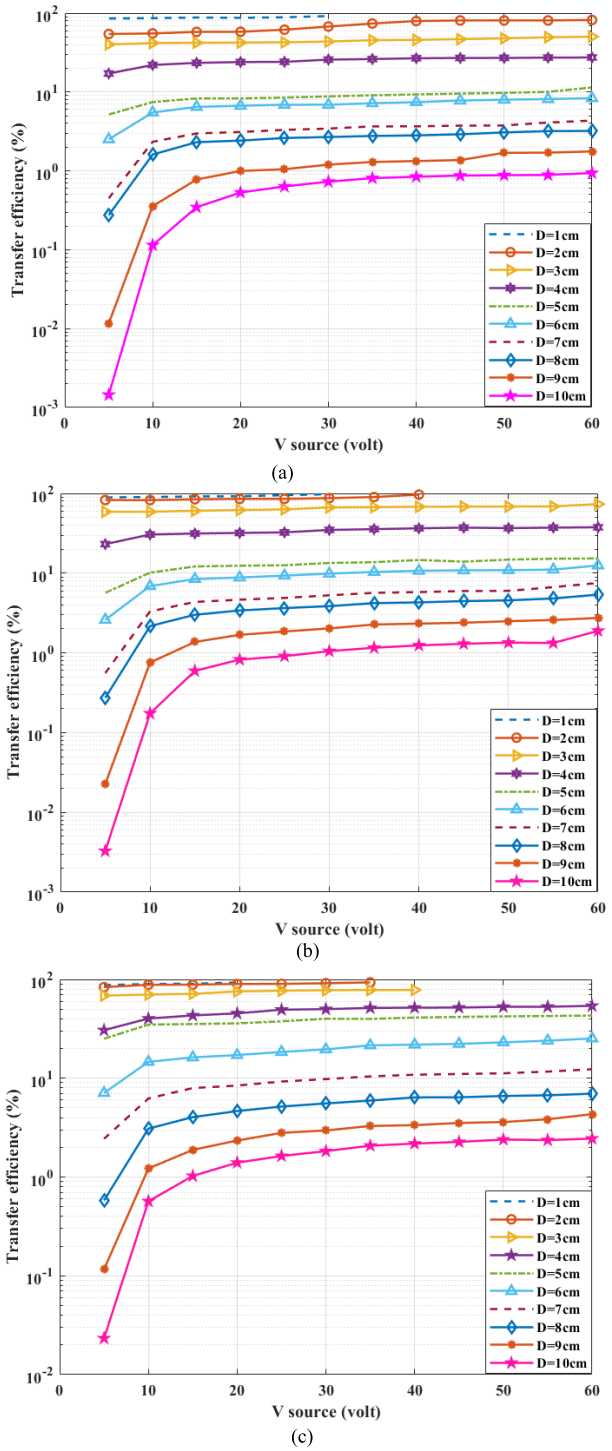

FIGURE 8. Transfer efficiency corresponds to different input voltages for transfer distances ranging from 1-10 cm at different resistive loads: (a) 50Ω, (b) 100Ω, and (c) 150Ω.

The measurement was recorded at a different transfer distance between the transmitter and receiver, ranging from 1-10 cm.

Fig. 7 shows that the x-axis represents the applied voltage source in volts, while the y-axis denotes the calculated delivered output power in watts. The delivered output power was calculated for three loads: 50 Ω, 100 Ω, and 150 Ω, as shown in Fig. 7a, 7b, and 7c, respectively. Fig. 7a shows that when the proposed SWC-MRC system has a 50-Ω resistive load, the delivered output power is 4.059 W at a transfer distance of 2 cm, and the V_{source} is 30 V. Whereas, we found that the delivered output power is 17.69 W at 2 cm when the V_{source} increased to 60 V. Fig. 7b and 7c show that the delivered output power was 7.956 W and 9.805 W with an air gap of 2 cm and a V_{source} of 30 V when the proposed SWC-MRC is loaded with 100 Ω and150 Ω, respectively. The delivered output power was 10.5825 W and 7.2603 W, respectively, with an air gap of 3 cm to 4 cm and a V_{source} of 60 V when the proposed SWC-MRC was loaded with 100 Ω and 150 Ω. The delivered power was decreased to 0.066 W, 0.129 W, and 0.177 W at 10 cm and with a V_{source} of 60 V for 50 Ω, 100 Ω, and 150 Ω as shown in Fig. 7a, 7b, and 7c, respectively. However, the delivered power was decreased to 0.012 W, 0.017 W, and 0.033 W at 10 cm and with a V_{source} of 30 V for 50 Ω, 100 Ω, and 150 Ω, respectively, as shown in Fig. 7a, 7b, and 7c. In this context, the delivered power of 0.612 V, 0.375V, and 0.311W can be achieved for 6 cm, 8 cm, and 9 cm at 50 Ω (Fig. 7a), 100 Ω (Fig. 7b), and 150 Ω (Fig. 7c), respectively, when the V_{source} is 60 V. This result fits the requirement for BMIs with low-power consumption as recommended in [57], [58].

C. RESULTS OF TRANSFER EFFICIENCY

For the proposed SWC-MRC system, the transfer efficiency is considered a vital metric to investigate system performance. Three different loads were used to check the transfer efficiency, as demonstrated in Fig. 8. The transfer efficiency was calculated according to equation 7 in section 5 as mentioned earlier, variables of the voltage source, transfer distance, and load were considered in our experiments. Fig. 8 shows that the x-axis represents the applied voltage source in volts, while the y-axis indicates the percentage of transfer efficiency. As shown in Fig. 8, the transfer efficiency decreases when the distance increases.

Fig. 8a reveals that the maximum transfer efficiency was 91.86% obtained at a 1-cm air gap when the proposed SWC-MRC system was loaded with 50 Ω and a supply of 30 V. In addition, the minimum transfer efficiency is 0.73% at further distances of 10 cm at the same V_{source}. Moreover, when the V_{source} is 60 V, the maximum and minimum transfer efficiencies are 81.90% and 0.94% at 2 and 10 cm, respectively. The maximum transfer efficiency was developed to 97.91% at a 1-cm air gap when a V_{source} of 30 V and resistive load of 100 Ω were adopted as shown in Fig. 8b. Conversely, the transfer efficiency deteriorates to 1.05% when a 10-cm air gap is considered. Here, the maximum and minimum transfer efficiencies were 92.99% and 1.39% at 1 cm and a V_{source} of 20 V, respectively, when the system is loaded by 150 Ω as shown in Fig. 8c. The DC output voltage of 5 V was achieved at transfer efficiencies of 8.36%, 5.38%, and 4.32% corresponding to 6 cm, 8 cm, and 9 cm for 50 Ω (Fig. 8a), 100 Ω (Fig. 8b), and 150 Ω (Fig. 8c) at a V_{source} of 60 V, respectively.

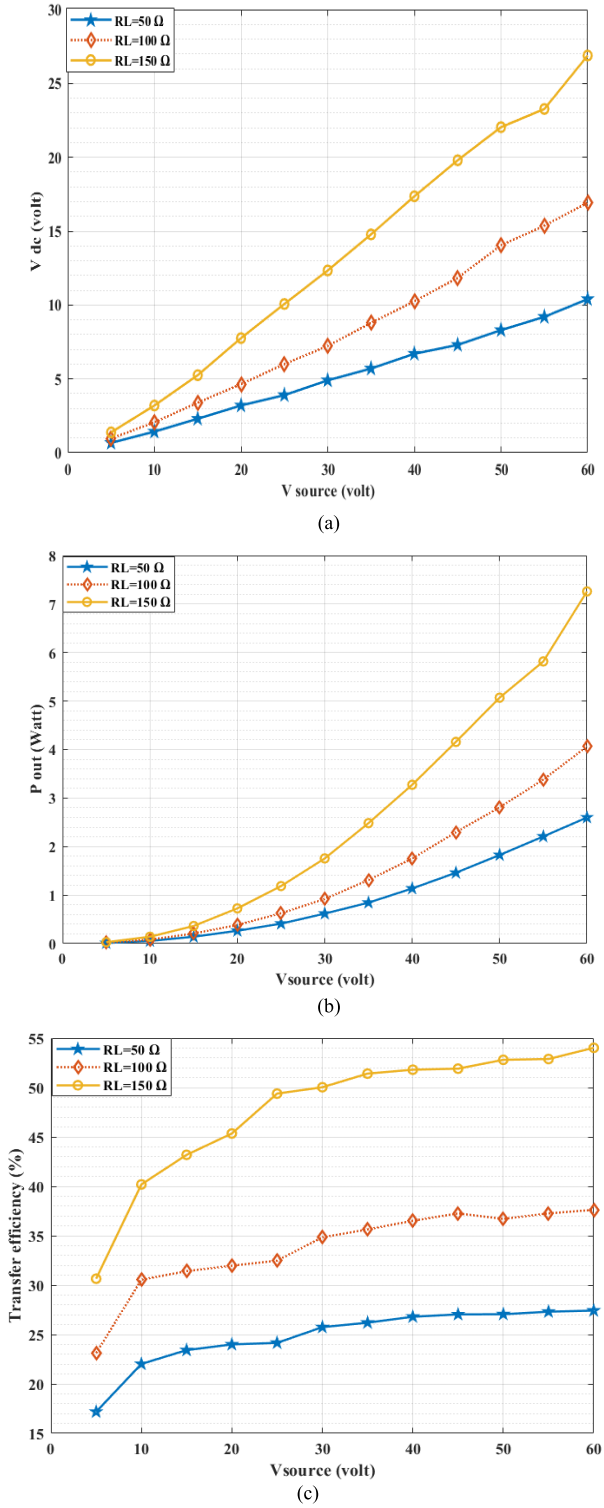

FIGURE 9. The effect of resistor loads 50 Ω, 100 Ω, and 150 Ω with an air gap of 4 cm on (a) DC output voltage, (b) delivered output power, and (c) transfer efficiency.

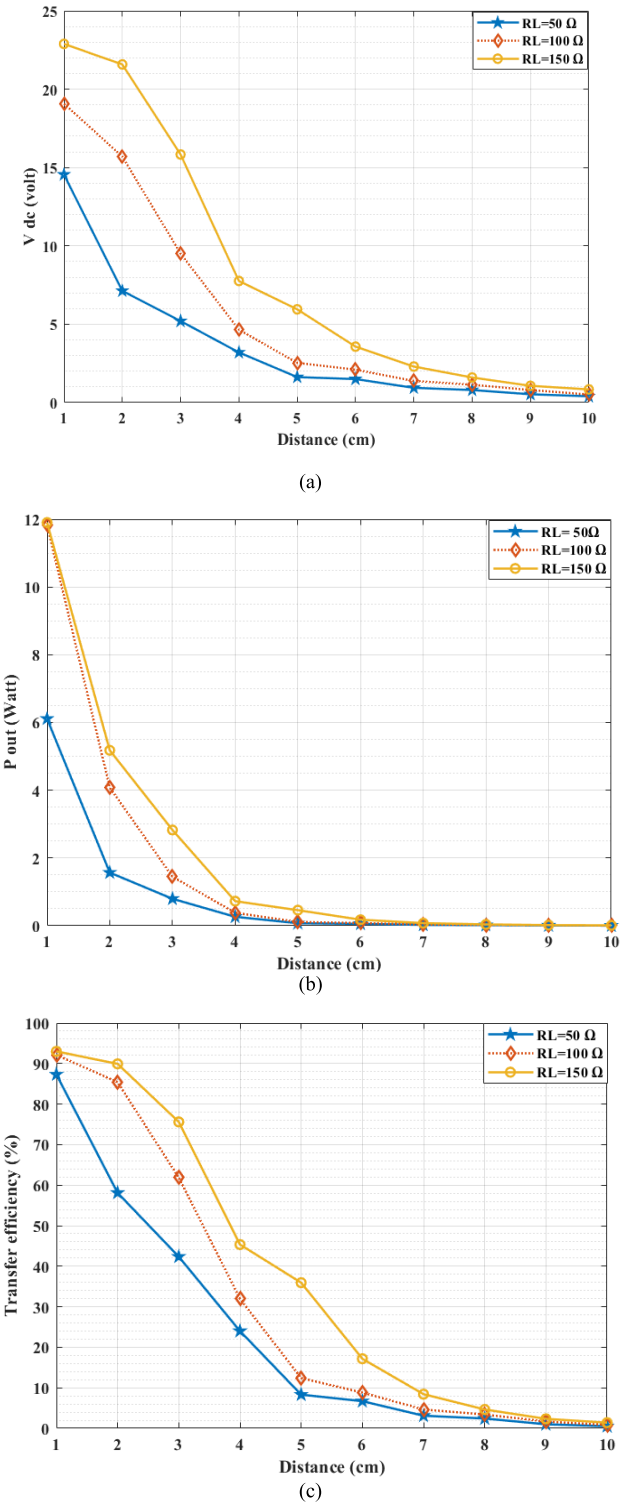

FIGURE 10. The effect of resistor load (50 Ω, 100 Ω, and 150 Ω) at air gaps ranging from 1-10 cm at 20 V on (a) DC output voltage, (b) delivered power, and (c) transfer efficiency.

VIII. COMPARISON RESULTS OF PERFORMANCE METRICS

From the aforementioned results, the performance metrics of the proposed SWC-MRC can be compared in terms of different loads (i.e., 50 Ω, 100 Ω, and 150 Ω) when a 4-cm distance between transfer and receiver coils is considered, as shown in Fig. 9.

A transfer distance of 4 cm was selected because the DC output voltage could be measured for all the values of V_{source},

TABLE 2. Comparison between performance metrics from previous studies and this work.

Ref. /Year	Frequency (MHz)	Configuration	Type of coil		Transfer distance (cm)	Efficiency (%)	Delivered power (mW)
			Transmitter	Receiver			
[27]/ 2020	8	NA	PCB Solenoid	PCB Solenoid	20	0.8	4.3
[34]/ 2020	6.78	S/P	PCB	PCB	1	24	NA
					0	44.5	NA
[35]/2017	6.78	S/S	Spiral	Spiral	1.5	36.43	500
[36]/ 2020	6.78	S/P	PCB	PCB	NA	10	NA
[37]/2018	13.56	S/P	Circular	Elliptical	0.5	3.65	26.64
					5	0.044	0.361
[41]/2019	13.56	S/P	PSC	PSC	0.5	75.1	157.7
					5	10.67	22.4
[42]/ 2020	13.56	NA	Circular and Spiral	Circular and Spiral	0.6	35	70
[59]/2017	0.246	NA	Modified Helmholtz coil	Mixed resonance scheme	NA	4.93	534
[60]/2019	4	P/P	PCB	PCB	0.5	0.15	NA
					1	0.08	NA
[61]/2020	0.067	P/P	FSC	MLCWC	0	23.37	1,680
					3	1.45	104
					6	0.012	8
SWC-MRC	6.78	S/P	Spider Web–Coil	Spider Web–Coil	1–10	97.91@ 1cm	23,500@1 cm
						93.38@ 2cm	12,420@2 cm

NA: Not available; PCB: printed circuit board, PSC: printed spiral coil; MLCWC: multi-layers copper wire coil; FSC: flat spiral coil

and the effect of coil heat diminishes at this distance. Hence, the delivered output power and transfer efficiency could be determined easily. Fig. 9a, 9b, and 9c illustrate the comparison of DC output voltage, delivered output power, and transfer efficiency, respectively, according to the change in applied V_{source} within a fixed distance (i.e., 4 cm). All figures disclosed to indicate the best performance in terms of DC output voltage was obtained at a 150-Ω resistive load, while the worst case was found at a 50-Ω resistive load.

The performance of the SWC-MRC for the selected distance (i.e., 4 cm) at 5-V DC demonstrated a delivered output power of 0.617 W, 0.625 W, and 0.362 W and a transfer efficiency of 25.74%, 32.47%, and 43.18% at 50 Ω (Fig. 9a), 100 Ω (Fig. 9b), and 150 Ω (Fig. 9c) when the V_{source} was 30 V, 25 V, and 15 V, respectively. The achieved result is appropriate for charging and satisfies the requirement for BMIs with low power consumption, such as cardiac pacemakers and neural implants.

Finally, the performance metrics of the proposed SWC-MRC can be examined for different distances with three loads (i.e., 50 Ω, 100 Ω, and 150 Ω) when 20 V of the V_{source} was adopted as presented in Fig. 10. The amount of 20 V was chosen because the measurements were stable at this voltage, and the effect of heat is lessened. The performance of the SWC-MRC for the chosen voltage (i.e., 20 V) and at 5-V DC power demonstrated a delivered output power of 0.7961 W, 1.447 W, and 0.459 W, respectively. Transfer efficiencies of 42.34%, 61.85%, and 35.93% were noted at 50 Ω (Fig. 10a), 100 Ω (Fig. 10b), and 150 Ω (Fig. 10c) when air gaps were 3 cm, 4 cm, and 5 cm, respectively.

IX. COMPARISON WITH PREVIOUS WORK

The performance metrics obtained from the proposed SWC-MRC system can be compared with the metrics of other scholars. A simple comparison with previous research utilizing wireless power transfer in biomedical sensors and implants was accomplished. In BMI applications, most of the presented related work has used different coil geometry such as spiral, Helmholtz, and other coils. The spider-web coil of our proposed system is rarely used in BMI applications.

The comparison involves many metrics such as operating frequency, coil type, transfer distance, delivered power, and transfer efficiency among various configurations as presented in Table 2. The table reveals that the performance metrics of the previous studies for different transfer distances between the transmitter and receiver coils were compared with those of the proposed SWC-MRC system to confirm the performance of the proposed system. The comparison shows that the maximum transfer efficiency in the proposed work is 97.91% at a 1-cm air gap when the V_{source} is 30 V and the resistive load is 100 Ω. In addition, the transfer efficiency was 93.38% at a 2-cm air gap between transmitter and receiver coils when the V_{source} is 35 V and the resistive load is 150 Ω. Moreover, the delivered power was 12.42 W at the same distance, V_{source}, and resistive load where this power is adequate to supply BMI such as LVADs, deep biomedical implants, and cochlear prostheses with power.

X. CONCLUSION

Sensors and BMI are crucial in monitoring, diagnosis, and therapeutic application in recent medical and healthcare

developments. Power supply and energy consumption are some of the challenges facing the use of these devices and sensors. Wireless power transfer is one of the solutions for overcoming battery capacity and charging problems. Wireless power transfer, specifically MRC, plays an essential part in wirelessly charging implantable biomedical systems such as pacemakers and cochlear prostheses. A design and implementation of SWC-MRC with an S/P configuration to a wirelessly charged BMI system for various input supply and different transfer distances between the transmitter and receiver coils for three cases of loads 50 Ω, 100 Ω, and 150 Ω have been investigated. A spider coil with a 20-AWG coil diameter was designed for both transmitter and receiver coils. The SWC-MRC implementation has been examined in an air medium without evaluating the human body nor electromagnetic field safety. We observed that the increase in the resistive load value resulted in improved delivery of power and efficiency at a larger transfer distance at the same input voltage. Also, the system efficiency decreases as the air gap between transmitter and receiver increases for the same input voltage. Moreover, the S/P configuration for asymmetrical coil succeeds in achieving adequate 5-V DC output for supplying voltage to the load or biomedical implant across a 2-cm air gap between transmitter and receiver coil. Future work will use another configuration to optimize output voltage and transfer efficiency as well as transfer power has given a larger range of transfer distance.

The current research did not consider the human tissue because it requires several extensive experiments to reduce the receiving coil size. A future task of this research will be to reduce the coil size of the receiver to be more convenient when it implants in animal tissues and even in human tissue.

REFERENCES

[1] A. Ballo, M. Bottaro, and A. D. Grasso, "A review of power management integrated circuits for ultrasound-based energy harvesting in implantable medical devices," *Appl. Sci.*, vol. 11, no. 6, p. 2487, Mar. 2021, doi: 10.3390/app11062487.

[2] J. Ausra, S. J. Munger, A. Azami, A. Burton, R. Peralta, J. E. Miller, and P. Gutruf, "Wireless battery free fully implantable multimodal recording and neuromodulation tools for songbirds," *Nature Commun.*, vol. 12, no. 1, pp. 1–12, Dec. 2021, doi: 10.1038/s41467-021-22138-8.

[3] A. Zurbuchen, A. Haeberlin, A. Pfenniger, L. Bereuter, J. Schaerer, F. Jutzi, C. Huber, J. Fuhrer, and R. Vogel, "Towards batteryless cardiac implantable electronic devices—The Swiss way," *IEEE Trans. Biomed. Circuits Syst.*, vol. 11, no. 1, pp. 78–86, Feb. 2017, doi: 10.1109/TBCAS.2016.2580658.

[4] H.-P. Phan, "Implanted flexible electronics: Set device lifetime with smart nanomaterials," *Micromachines*, vol. 12, no. 2, p. 157, Feb. 2021, doi: 10.3390/mi12020157.

[5] A. M. Jawad, R. Nordin, S. K. Gharghan, H. M. Jawad, and M. Ismail, "Opportunities and challenges for near-field wireless power transfer: A review," *Energies*, vol. 10, no. 7, pp. 1–11, 2017, doi: 10.3390/en10071022.

[6] R. Shadid and S. Noghanian, "A literature survey on wireless power transfer for biomedical devices," *Int. J. Antennas Propag.*, vol. 2018, Jan. 2018, Art. no. 4382841, doi: 10.1155/2018/4382841.

[7] M. A. Houran, X. Yang, and W. Chen, "Magnetically coupled resonance WPT: Review of compensation topologies, resonator structures with misalignment, and EMI diagnostics," *Electronics*, vol. 7, no. 11, p. 296, 2018, doi: 10.3390/electronics7110296.

[8] T. Campi, S. Cruciani, V. De Santis, F. Maradei, and M. Feliziani, "Near field wireless powering of deep medical implants," *Energies*, vol. 12, no. 14, p. 2720, Jul. 2019, doi: 10.3390/en12142720.

[9] H. Qiang, X. Huang, L. Tan, and H. Huang, "Study on topology design of wireless power transfer for Electric Vehicle based on magnetic resonance coupling," *Adv. Mater. Res.*, vols. 308–310, pp. 1000–1003, Apr. 2011, doi: 10.4028/www.scientific.net/AMR.308-310.1000.

[10] D. Sun, M. Chen, S. Podilchak, A. Georgiadis, Q. S. Abdullahi, R. Joshi, S. Yasin, J. Rooney, and J. Rooney, "Investigating flexible textile-based coils for wireless charging wearable electronics," *J. Ind. Textiles*, vol. 50, no. 3, pp. 333–345, Sep. 2020, doi: 10.1177/1528083719831086.

[11] Y. Liu, Y. Li, J. Zhang, S. Dong, C. Cui, and C. Zhu, "Design a wireless power transfer system with variable gap applied to left ventricular assist devices," in *Proc. IEEE PELS Workshop Emerg. Technol., Wireless Power Transf. (Wow)*, Montreal, QC, Canada, Jun. 2018, pp. 1–5, doi: 10.1109/WoW.2018.8450655.

[12] M. F. Mahmood, S. L. Mohammed, S. K. Gharghan, A. Al-Naji, and J. Chahl, "Hybrid coils-based wireless power transfer for intelligent sensors," *Sensors*, vol. 20, no. 9, p. 2549, Apr. 2020, doi: 10.3390/s20092549.

[13] L. Gu and J. Rivas-Davila, "1.7 kW 6.78 MHz wireless power transfer with air-core coils at 95.7% DC-DC efficiency," in *Proc. IEEE Wireless Power Transf. Conf.*, San Diego, CA, USA, Jun. 2021, pp. 1–4, doi: 10.1109/WPTC51349.2021.9458037.

[14] S.-H. Hwang, C. Kang, Y.-H. Son, and B.-J. Jang, "Software-based wireless power transfer platform for various power control experiments," *Energies*, vol. 8, no. 8, pp. 7677–7689, Jul. 2015, doi: 10.3390/en8087677.

[15] J. Wu, C. Zhao, Z. Lin, J. Du, Y. Hu, and X. He, "Wireless power and data transfer via a common inductive link using frequency division multiplexing," *IEEE Trans. Ind. Electron.*, vol. 62, no. 12, pp. 7810–7820, Dec. 2015, doi: 10.1109/TIE.2015.2453934.

[16] X. Ge, L. Cheng, Y. Yao, and W.-H. Ki, "A 6.78 MHz single-stage wireless power transmitter using a 3-mode zero-voltage switching class-D PA," *IEEE Trans. Circuits Syst. I, Reg. Papers*, vol. 68, no. 6, pp. 2736–2748, Jun. 2021, doi: 10.1109/TCSI.2021.3071265.

[17] J. Yang, Y. Shi, W. Y. Wei, and H. Shen, "A wireless power transfer system based on impedance matching network," *Int. J. RF Microw. Comput.-Aided Eng.*, vol. 30, no. 12, Dec. 2020, Art. no. e22437, doi: 10.1002/mmce.22437.

[18] Q. Wang, W. Che, M. Dionigi, F. Mastri, M. Mongiardo, and G. Monti, "Gains maximization via impedance matching networks for wireless power transfer," *Prog. Electromagn. Res.*, vol. 164, pp. 135–153, 2019, doi: 10.2528/PIER18102402.

[19] M. Al-Saadi, S. Valtchev, L. Romba, J. Gonçalves, and A. Cráciunescu, "Comparison of spiral and square coil configurations in wireless power transfer system for contactless battery charging," in *Proc. Electr. Veh. Int. Conf.*, Bucharest, Romania, Oct. 2019, pp. 1–5, doi: 10.1109/EV.2019.8892897.

[20] B. H. Waters, J. Park, J. C. Bouwmeester, J. Valdovinos, A. Geirsson, A. P. Sample, J. R. Smith, and P. Bonde, "Electrical power to run ventricular assist devices using the free-range resonant electrical energy delivery system," *J. Heart Lung Transplantation*, vol. 37, no. 12, pp. 1467–1474, Dec. 2018, doi: 10.1016/j.healun.2018.08.007.

[21] T. Campi, S. Cruciani, F. Maradei, and M. Feliziani, "Coil design of a wireless power-transfer receiver integrated into a left ventricular assist device," *Electronics*, vol. 10, no. 8, p. 874, Apr. 2021, doi: 10.3390/electronics10080874.

[22] M. Haerinia and R. Shadid, "Wireless power transfer approaches for medical implants: A review," *Signals*, vol. 1, no. 2, pp. 209–229, Dec. 2020, doi: 10.3390/signals1020012.

[23] K. Gharghan and S. Fakhrulddin, "Energy-efficient elderly fall detection system based on power reduction and wireless power transfer," *Sensors*, vol. 19, no. 20, p. 4452, Oct. 2019, doi: 10.3390/s19204452.

[24] M. F. Mahmood, S. L. Mohammed, S. K. Gharghan, and S. L. Zubaidi, "Wireless power transfer based on spiral–spider coils for a wireless heart rate sensor," in *Proc. 13th Int. Conf. Develop. Systems Eng. (DeSE)*, Liverpool, U.K., Dec. 2020, pp. 183–188, doi: 10.1109/DeSE51703.2020.9450775.

[25] S. Guo, P. Zhang, J. Guo, L. Wang, and G. Sun, "Design of wireless power transmission system based on magnetic coupling resonant for the capsule endoscopy," in *Proc. IEEE Int. Conf. Mechatronics Autom.*, Takamatsu, Japan, Jun. 2017, pp. 23–28, doi: 10.1109/ICMA.2017.8015782.

[26] T. Campi, S. Cruciani, F. Maradei, and M. Feliziani, "Wireless power supply system for left ventricular assist device and implanted cardiac defibrillator," in *Proc. IEEE Wireless Power Transf. Conf.*, San Diego, CA, USA, Jun. 2021, pp. 1–4, doi: 10.1109/WPTC51349.2021.9458163.

[27] L. Huang, A. Murray, and B. W. Flynn, "Optimal design of a 3-coil wireless power transfer system for deep micro-implants," *IEEE Access*, vol. 8, pp. 193183–193201, 2020, doi: 10.1109/ACCESS.2020.3031960.

[28] K. L. Montgomery, A. J. Yeh, J. S. Ho, V. Tsao, S. M. Iyer, L. Grosenick, E. A. Ferenczi, Y. Tanabe, K. Deisseroth, S. L. Delp, and A. S. Y. Poon, "Wirelessly powered, fully internal optogenetics for brain, spinal and peripheral circuits in mice," *Nat. Methods*, vol. 12, no. 10, pp. 969–974, 2015, doi: 10.1038/nmeth.3536.

[29] L. Zhao, D. Thrimawithana, and U. K. Madawala, "Hybrid bidirectional wireless EV charging system tolerant to pad misalignment," *IEEE Trans. Ind. Electron.*, vol. 64, no. 9, pp. 7079–7086, Sep. 2017, doi: 10.1109/TIE.2017.2686301.

[30] G. Guidi and J. A. Suul, "Minimizing converter requirements of inductive power transfer systems with constant voltage load and variable coupling conditions," *IEEE Trans. Ind. Electron.*, vol. 63, no. 11, pp. 6835–6844, Nov. 2016, doi: 10.1109/TIE.2016.2582459.

[31] M. Saad, A. H. Mahammad, A. S. Salina, and H. Aini, "Analysis and optimization of spiral circular inductive coupling link for bio-implanted applications on air and within human tissue," *Sensors*, vol. 14, no. 7, pp. 11522–11541, Jun. 2014, doi: 10.3390/s140711522.

[32] X. Mou, D. T. Gladwin, R. Zhao, and H. Sun, "Survey on magnetic resonant coupling wireless power transfer technology for electric vehicle charging," *IET Power Electron.*, vol. 12, no. 12, pp. 3005–3020, 2019, doi: 10.1049/iet-pel.2019.0529.

[33] M. Al-Saadi and S. Valtchev, "New analytical formulas for coupling coefficient of two inductively coupled ring coils in inductive wireless power transfer system," *Soc. Telecommun. Eng. LNICST*, vol. 333, no. 2, pp. 117–127, 2020, doi: 10.1007/978-3-030-62483-5_13.

[34] D. Kim, D. Jeong, J. Kim, H. Kim, J. Kim, S.-M. Park, and S. Ahn, "Design and implementation of a wireless charging-based cardiac monitoring system focused on temperature reduction and robust power transfer efficiency," *Energies*, vol. 13, no. 4, p. 1008, Feb. 2020, doi: 10.3390/en13041008.

[35] S. Peng, M. Liu, Z. Tang, and C. Ma, "Optimal design of megahertz wireless power transfer systems for biomedical implants," in *Proc. IEEE 26th Int. Symp. Ind. Electron. (ISIE)*, Edinburgh, U.K., Jun. 2017, pp. 805–810, doi: 10.1109/ISIE.2017.8001349.

[36] J. Kim, H. Kim, D. Kim, H.-J. Park, K. Ban, S. Ahn, and S.-M. Park, "A wireless power transfer based implantable ECG monitoring device," *Energies*, vol. 13, no. 4, p. 905, Feb. 2020, doi: 10.3390/en13040905.

[37] J.-C. Heo, J. Park, S. Kim, J. Ku, and J.-H. Lee, "Development and application of wireless power transmission systems for wireless ECG sensors," *J. Sensors*, vol. 2018, pp. 1–7, Dec. 2018, doi: 10.1155/2018/5831056.

[38] S. J. M. Yazdi, S. Cho, and J.-H. Lee, "Analysis and optimization of six types of two-coil inductive for the human implantable wireless electrocardiogram sensor," *Proc. SPIE Opt. Fibers Sensors Med. Diag., Treatment Environ. Appl.*, vol. 11635, Oct. 2021, Art. no. 116350, doi: 10.1117/12.2582372.

[39] S. Dubey and J. C. Chiao, "Power transfer for a flexible gastric stimulator," in *Proc. IEEE Topical Conf. Biomed. Wireless Technol., Netw., Sens. Syst.*, Austin, TX, USA, Jan. 2016, pp. 15–17, doi: 10.1109/BIOWIRELESS.2016.7445549.

[40] C. Cui, Q. Zhao, and Z. Li, "Design of wireless power supply optimized structure for capsule endoscopes," *J. Power Technol.*, vol. 96, no. 2, pp. 101–109, 2016.

[41] Y. Ben Fadhel, S. Ktata, K. Sedraoui, S. Rahmani, and K. Al-Haddad, "A modified wireless power transfer system for medical implants," *Energies*, vol. 12, no. 10, p. 1890, May 2019, doi: 10.3390/en12101890.

[42] D. Xu, Q. Zhang, and X. Li, "Implantable magnetic resonance wireless power transfer system based on 3D flexible coils," *Sustainability*, vol. 12, no. 10, p. 4149, May 2020, doi: 10.3390/su12104149.

[43] A. Ibrahim and M. Kiani, "Inductive power transmission to millimeter-sized biomedical implants using printed spiral coils," in *Proc. Annu. Int. Conf. Eng. Med. Biol. Soc.*, Orlando, FL, USA, Aug. 2016, pp. 4800–4803, doi: 10.1109/EMBC.2016.7591801.

[44] O. Knecht, R. Bosshard, and J. W. Kolar, "High-efficiency transcutaneous energy transfer for implantable mechanical heart support systems," *IEEE Trans. Power Electron.*, vol. 30, no. 11, pp. 6221–6236, Nov. 2015, doi: 10.1109/TPEL.2015.2396194.

[45] R. Shadid, M. Haerinia, S. Roy, and S. Noghanian, "Hybrid inductive power transfer and wireless antenna system for biomedical implanted devices," *Prog. Electromagn. Res. C*, vol. 88, pp. 77–88, 2018, doi: 10.2528/PIERC18061604.

[46] M. Haerinia and S. Noghanian, "A printed wearable dual-band antenna for wireless power transfer," *Sensors*, vol. 19, no. 7, p. 1732, Apr. 2019, doi: 10.3390/s19071732.

[47] J. Sallan, J. L. Villa, A. Llombart, and J. F. Sanz, "Optimal design of ICPT systems applied to electric vehicle battery charge," *IEEE Trans. Ind. Electron.*, vol. 56, no. 6, pp. 2140–2149, Jun. 2009, doi: 10.1109/TIE.2009.2015359.

[48] M. A. Houran, X. Yang, W. Chen, and M. Samizadeh, "Wireless power transfer: Critical review of related standards," in *Proc. Int. Power Electron. Conf.*, Niigata, Japan, May 2018, pp. 1062–1066, doi: 10.23919/IPEC.2018.8507837.

[49] Development Board EPC9065. *6.78 MHz, High Power ZVS Class-D Development Board*. Accessed: Aug. 12, 2020. [Online]. Available: https://epcco.com/epc/Portals/0/epc/documents/guides/EPC9065_qsg.pdf

[50] J. Wang, M. Leach, E. G. Lim, Z. Wang, and Y. Huang, "Investigation of magnetic resonance coupling circuit topologies for wireless power transmission," *Microw. Opt. Technol. Lett.*, vol. 61, no. 7, pp. 1755–1763, 2019, doi: 10.1002/mop.31803.

[51] P. Abiri, A. Abiri, R. R. S. Packard, Y. Ding, A. Yousefi, J. Ma, M. Bersohn, K.-L. Nguyen, D. Markovic, S. Moloudi, and T. K. Hsiai, "Inductively powered wireless pacing via a miniature pacemaker and remote stimulation control system," *Sci. Rep.*, vol. 7, no. 1, Dec. 2017, Art. no. 6187, doi: 10.1038/s41598-017-06493-5.

[52] M. A. Hussain, S. K. Gharghan, and H. Q. Hamood, "Single tube copper coil via strong coupling wireless power transfer for low power devices," *J. Adv. Res. Dyn. Control Syst.*, vol. 11, no. 1, Special Issue, pp. 1818–1827, 2019.

[53] M. Rehman, P. Nallagownden, and Z. Baharudin, "Efficiency investigation of SS and SP compensation topologies for wireless power transfer," *Int. J. Power Electron. Drive Syst.*, vol. 10, no. 4, pp. 2157–2164, 2019, doi: 10.11591/ijpeds.v10.i4.2157-2164.

[54] L. Murliky, R. W. Porto, V. J. Brusamarello, F. Rangel de Sousa, and A. Triviño-Cabrera, "Active tuning of wireless power transfer system for compensating coil misalignment and variable load conditions," *AEU-Int. J. Electron. Commun.*, vol. 119, May 2020, Art. no. 153166, doi: 10.1016/j.aeue.2020.153166.

[55] M. F. Mahmood, S. L. Mohammed, and S. K. Gharghan, "Free battery-based energy harvesting techniques for medical devices," in *IOP Conf. Ser., Mater. Sci. Eng.*, vol. 745, no. 1, Dec. 2019, Art. no. 12094, doi: 10.1088/1757-899X/745/1/012094.

[56] M. F. Mahmood, S. K. Gharghan, S. L. Mohammed, A. Al-Naji, and J. Chahl, "Design of powering wireless medical sensor based on spiral-spider coils," *Designs*, vol. 5, no. 4, p. 59, Sep. 2021, doi: 10.3390/designs5040059.

[57] C.-Y. Tsui, "Energy harvesting and power delivery for implantable medical devices," *Found. Trends Electron. Design Autom.*, vol. 7, no. 3, pp. 179–246, 2013, doi: 10.1561/1000000029.

[58] A. Zebda, J.-P. Alcaraz, P. Vadgama, S. Shleev, S. D. Minteer, F. Boucher, P. Cinquin, and D. K. Martin, "Challenges for successful implantation of biofuel cells," *Bioelectrochemistry*, vol. 124, pp. 57–72, Dec. 2018, doi: 10.1016/j.bioelechem.2018.05.011.

[59] M. R. Basar, M. Y. Ahmadm, J. Cho, and F. Ibrahim, "Stable and high-efficiency wireless power transfer system for robotic capsule using a modified Helmholtz coil," *IEEE Trans. Ind. Electron.*, vol. 64, no. 2, pp. 1113–1122, Feb. 2017, doi: 10.1109/TIE.2016.2614268.

[60] M. Sinclair, D. Biswas, T. L. J. Hyde, I. Mahbub, L. Chang, and Y. Hao, "Design of a flexible receiver module for implantable wireless power transfer (WPT) applications," in *Proc. United States Nat. Committee URSI Nat. Radio Sci. Meeting*, Boulder, CO, USA, Jan. 2019, pp. 1–2, doi: 10.23919/USNC-URSI-NRSM.2019.8713015.

[61] M. A. Hussain, S. K. Gharghan, and H. Q. Hamood, "Design and implementation of wireless low-power transfer for medical implant devices," in *IOP Conf. Ser., Mater. Sci. Eng.*, vol. 745, no. 1, pp. 16–17, Dec. 2019, doi: 10.1088/1757-899X/745/1/012087.

AMAL IBRAHIM MAHMOOD received the B.Sc. and M.Sc. degrees in biomedical engineering from Al-Nahrain University, Iraq, in 2005 and 2009, respectively. She is currently pursuing the Ph.D. degree with the Biomedical Engineering Department, Faculty of Engineering, Helwan University, Cairo, Egypt. She is also a Lecturer with the Department of Medical Instrumentation Techniques Engineering, Electrical Engineering Technical College, Middle Technical University (MTU), Baghdad, Iraq. Her research interests include optical fibers, biomedical sensors, and wireless power transfer applications in the biomedical implant.

SADIK KAMEL GHARGHAN (Member, IEEE) received the B.Sc. degree in electrical and electronics engineering and the M.Sc. degree in communication engineering from the University of Technology, Iraq, in 1990 and 2005, respectively, and the Ph.D. degree in communication engineering from Universiti Kebangsaan Malaysia (UKM), Malaysia, in 2016. He is currently with the Department of Medical Instrumentation Techniques Engineering, Electrical Engineering Technical College, Middle Technical University, Baghdad, Iraq, as a Professor. His research interests include energy-efficient wireless sensor networks, biomedical sensors, microcontroller applications, WSN localization based on artificial intelligence techniques and optimization algorithms, indoor and outdoor path loss modeling, harvesting technique, wireless power transfer, jamming on direct sequence spread spectrums, and drone in medical applications.

MOHAMED A. A. ELDOSOKY received the B.Sc. degree in communication and electronics from Helwan University, in 1997, the master's degree in microstrip antennas, in 2000, and the Ph.D. degree in biomedical engineering in the application of ultrasonic tomography, in 2005. From 2005 to 2011, he became an Assistant Professor in biomedical engineering. Since 2016, he has been a Professor in biomedical engineering with Helwan University. He has more than 70 publications in biomedical engineering.

MUSTAFA FALAH MAHMOOD received the B.Sc. degree in medical instrumentation techniques engineering from Middle Technical University (MTU), Baghdad, Iraq, in 2010, and the M.Sc. degree in medical instrumentation engineering techniques from the Electrical Engineering Technical College, Baghdad, in 2020. He is currently with the Department of Medical Instrumentation Engineering Techniques, Electrical Engineering Technical College, MTU, as an Assistant Teacher. His research interests include wireless energy transmission, alternative energy generation without the use of batteries, the design of medical devices with low cost and high efficiency, biomedical sensors, and microcontroller applications.

AHMED M. SOLIMAN received the B.Sc. degree (Hons.) in biomedical engineering from Helwan University, Helwan, Cairo, Egypt, in 2003, the M.S. degree in biotechnology engineering from the University of Chemical Technology and Metallurgy (UCTM), Sofia, Bulgaria, in 2009, and the M.S. and Ph.D. degrees in biomedical engineering from Helwan University, in 2010 and 2017, respectively. From 2010 to 2012, he was an exchange Ph.D. student with the Atomic Physics Division, Lund Medical Laser Centre, Biophotonics Group, Physics Department, Faculty of Engineering (LTH), Lund University, Lund, Sweden. He is currently an Assistant Professor with the Biomedical Engineering Department, Faculty of Engineering, Helwan University. His research interests include surface acoustic wave devices, microfluidics, biosensors, biotechnology engineering, medical optics, biomedical devices, neural networks, deep learning, and modeling and simulations in biomedical applications. He is also a Technical Examiner Member at Egyptian Patent Office.

He received fellowships for M.Sc. degree and exchange Ph.D. degree from Erasmus Mundus External Cooperation Window (EMECW) Program, in 2007 and 2010, respectively. Also, he received a fellowship from Swedish Institute Scholarship for Ph.D. studies—Guest Scholarship Program, Sweden, in 2012.